

Original Research

Differences in Stress Forces and Geometry between Left and Right Coronary Artery: A Pathophysiological Aspect of Atherosclerosis Heterogeneity

SOTIRIOS A. KATRANAS¹, ANASTASIOS L. KELEKIS², ANTONIOS P. ANTONIADIS¹, ANTONIOS G. ZIAKAS¹, GEORGE D. GIANNOGLOU¹

¹First Cardiology Department, ²Department of Radiology, AHEPA University General Hospital, Aristotle University Medical School, Thessaloniki, Greece

Key words:

Coronary computed tomography angiography, topography of atherosclerosis, endothelial shear stress, molecular viscosity, wall stress, curvature.

Manuscript received:
April 2, 2013;
Accepted:
September 10, 2014.

Address:

Sotirios A. Katranas

First Cardiology
Department
AHEPA University
General Hospital
Aristotle University
Medical School
1 Kyriakidi St.
54636 Thessaloniki,
Greece
sotiriskatranas@yahoo.com

Introduction: We sought to assess noninvasively the differences in hemorrheologic and geometric parameters between the left and right coronary artery (RCA). Low endothelial shear stress (ESS), high molecular viscosity (MV), and high wall stress (WS) induce atherosclerosis, while curvature and torsion have lately been implicated in the atherosclerotic process.

Methods: We studied 28 coronary arteries from 22 subjects undergoing coronary computed tomography angiography. We performed 3D reconstruction of the left anterior descending (LAD, n=14), left circumflex (LCx, n=5), and RCA (n=9) arteries. ESS, MV, and WS were calculated for 2-mm segments using computational fluid dynamics. Curvature and torsion were calculated for each segment using morphometric algorithms.

Results: A total length of 187 cm of coronary arteries was studied. ESS was higher in the LAD compared to the LCx and RCA (13.76 Pa vs. 3.49 Pa vs. 3.76 Pa, $p < 0.001$); MV was higher in the LCx compared to the LAD and RCA (0.00542 Pa·s vs. 0.00173 Pa·s vs. 0.00240 Pa·s, $p < 0.001$); and WS had higher values in the RCA compared to the LAD and LCx (289.98 mmHg vs. 255.93 mmHg vs. 235.18 mmHg, $p < 0.001$). Curvature was greater in the LCx compared to the LAD and RCA (0.1447 mm^{-1} vs. 0.1229 mm^{-1} vs. 0.1234 mm^{-1} , $p < 0.05$), while torsion was found not to differ among the coronary arteries.

Conclusions: Hemorrheologic and geometric parameters differ between the left and right coronary arteries. These factors, either alone or in association with local flow patterns and geometry, may affect the topography of atherosclerosis in the coronary arterial tree.

Epidemiological studies have found atherosclerosis to be non-uniformly distributed between the left and right coronary artery systems. A large retrospective study of 17,323 consecutive angiographies found left coronary artery (LCA)-only disease to be more frequent (35%) than right coronary artery (RCA)-only disease (6.5%).¹ An intravascular ultrasound study in young transplanted hearts demonstrated ath-

erosclerosis to be more frequently detected in the left anterior descending artery (LAD) compared to the left circumflex (LCx), with an intermediate incidence in the RCA, while a previous histopathological study in 2964 hearts showed that the LAD exhibited atherosclerosis more often than the RCA.^{2,3}

The entire coronary arterial tree is exposed to the same systematic risk factors; however, only specific areas exhibit ath-

erosclerotic lesions. It has been found that certain sites, such as bifurcations, inner areas of curvatures, and branch origins, are more prone to develop atherosclerosis than others. The effort to explain this preferential susceptibility to atherosclerosis has revealed the effects of hemorrheologic factors, among which endothelial shear stress (ESS) has a prominent role. Other hemorrheologic factors that have been studied include molecular viscosity (MV) and wall stress (WS), while geometric factors such as curvature and torsion have recently been drawing more attention.^{4,5}

The aim of this study was to evaluate any potential differences in hemorrheologic and geometrical factors between the left and right coronary arterial system that might account for the difference in the prevalence of atherosclerosis.

Methods

Study subjects

The study included 22 individuals (19 men, mean age 62 ± 12 years), who either underwent coronary computed tomography angiography (CCTA) for the investigation of suspected coronary artery disease with moderate or low risk or had known coronary artery disease, but were unable to undergo invasive coronary angiography. The characteristics of the study population are summarized in Table 1.

All procedures followed were in accordance with the ethical standards of the responsible committee on human experimentation (institutional and national) and with the Helsinki Declaration of 1975, as revised in 2008. Informed consent was obtained from all patients prior to their inclusion in the study.

Coronary CTA Protocol

CCTA (128-detector) was performed using a SOMATOM Definition AS+ device (Siemens, Germany). The arterial pressure was measured with an arm-band sphygmomanometer just before the examination. A bolus intravenous dose of iodine contrast was given through the basilic or cephalic vein (Ioversol, Optiray 350, Mallinckrodt Medical Imaging, Damastown, Mulhuddant, Ireland; dose 80 mL for body weight <80 kg, plus 5% per each 5 kg >80 kg). The scan timing was bolus tracking at flow rate 5 mL/s. The reconstruction thickness was 0.625 mm and the phase increment 10%. The acquisition technique

Table 1. Patient characteristics.

Demographics:	
Patients (n)	22
Age (years)	62 ± 3
Males	19 (86%)
Body mass index (kg/m ²)	28 ± 1
Heart rate (/min)	58 ± 2
Medical history (n):	
Myocardial infarction	3 (14%)
Arterial disease	5 (23%)
Risk Factors (n):	
Smoking	10 (45%)
Diabetes mellitus	6 (27%)
Hypercholesterolemia (>240 mg/dL)	13 (59%)
Arterial hypertension	14 (64%)
Positive family history	2 (9%)
Exercise (n)	13 (59%)
Drug treatment (n):	17 (77%)
Statins	11 (50%)
ω 3-fatty acids	2 (9%)
Beta-blockers	8 (36%)
Calcium channel blockers	4 (18%)
Angiotensin-converting enzyme inhibitors	5 (23%)
Diuretics	9 (41%)
Angiotensin receptor blockers	7 (32%)
Aspirin	8 (36%)
Clopidogrel	4 (18%)

was retrospective using an average of 1500-1850 dlp. The examination was ECG-gated and took place during hold inspiration. Subjects with heart rates >75 /min received propranolol 20-40 mg per os 15-30 minutes prior to the examination to achieve better image quality.⁶

3D coronary reconstruction

The major coronary arteries were reconstructed on the basis of the electrocardiogram with the use of MIMICS (Materialise Software, Belgium) based on DICOMs generated from the CCTA (Figure 1).⁷ The image quality was optimal in non-calcified as well as in mildly or moderately calcified plaques. Coronary arteries having intensely calcified plaques were not included in the study as the image quality was poor.

Segments of interest

By nature, coronary artery disease exhibits a mixed and heterogeneous distribution in the coronary arteries: i.e. diseased segments coexist with non-diseased. It is not, however, very clear whether the diseased segments behave distinctly differently from the non-

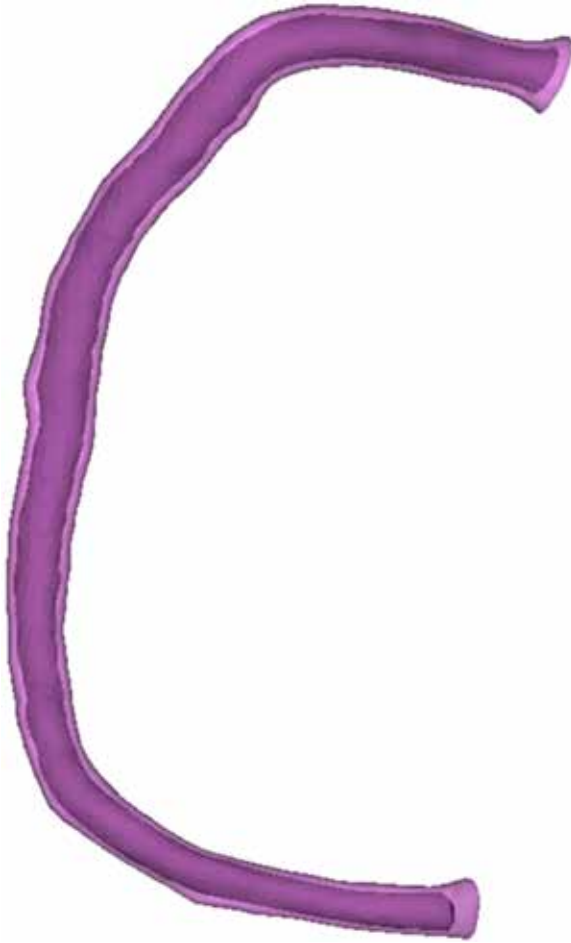


Figure 1. Three-dimensional reconstruction of a right coronary artery (both lumen and wall).

diseased ones in terms of the parameters studied; nor is the degree of influence between adjacent diseased and non-diseased segments fully understood. For these reasons, we considered that the presence of a diseased area in an artery does not render the entire artery diseased; thus, we employed a segment-based analysis using Rhinoceros (Robert McNeel & Associates, Seattle, USA), with a 2 mm-long segment as the basis of measurement. The segments were categorized as diseased or non-diseased according to the visual presence of atheroma; we analyzed the coronary segments both in total and separately (diseased versus non-diseased). In each segment, the radius and wall thickness were calculated.

Grid generation and computational fluid dynamics

In each reconstructed coronary artery, a computational grid was built and a finite-element unstructured

mesh with tetrahedral elements was employed for the lumen volume. Subsequently, the arterial models were imported to a computational solver (Fluent, Fluent Inc. Products, Lebanon, USA), where the ESS, MV, and wall pressure were calculated for each node of the computational mesh.⁸ We modeled blood as a non-Newtonian fluid with power-law index 0.7, minimum viscosity limit 0.0001 kg/(m·s), maximum viscosity limit 0.1 kg/(m·s), and a density of 1058 kg/m³. Steady laminar flow was assumed and at the inlet a velocity of 0.17 m/s was specified in accordance with the literature.⁹⁻¹⁰ At the flow outlet, zero pressure conditions were defined and the no-slip condition was applied at the wall, which was considered rigid.¹¹ Mean ESS, MV, and wall pressure values were calculated for each of the arterial segments (Figure 2).

Assessment of wall stress

Wall stress was calculated according to Laplace's Law:

$$T = \frac{P \times r}{d}$$

where P refers to wall pressure, r to radius, and d to wall thickness. Wall pressure was calculated using computational fluid dynamics, while radius and wall thickness were determined from morphometry measurements with Rhinoceros. Each variable was calculated in terms of mean values for each segment.

Assessment of curvature and torsion

Curvature and torsion were calculated by means of a special algorithm developed on Rhinoceros (Robert McNeel & Associates, Seattle, USA). Both curvature and torsion were calculated for each segment of interest.

Statistical analyses

Statistical calculations were performed using SPSS v17.0 (SPSS Inc., Chicago IL, USA). Categorical variables are summarized as absolute counts and percentages, and continuous variables as mean \pm standard error of the mean. The clustering of arterial 2-mm segments within patients introduces a systematic error, which was offset by using mixed-effects ANOVA where the patient and artery were designated as random effects. All statistical tests were two-tailed and statistical significance was defined as an alpha level ≤ 0.05 .

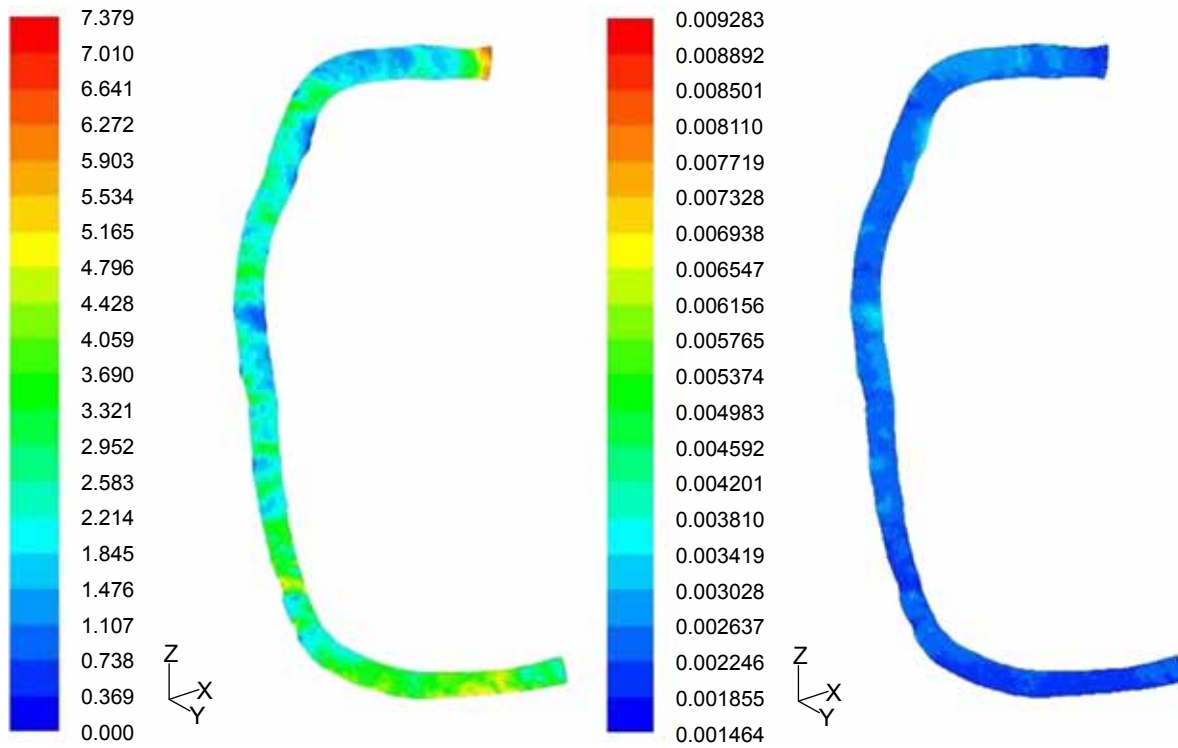


Figure 2. Endothelial shear stress (left) and molecular viscosity (right) in a right coronary artery using computational fluid dynamics.

Results

We reconstructed 28 arteries (LAD n=14, LCx n=5, RCA n=9) with a total length of 1.9 m. The remaining arteries were not reconstructed as they lacked high quality images. The mean length of each arterial reconstruction was 67 ± 6 mm. A total of 912 segments were identified, with 32% of them diseased and 68% normal. A total of 87 discrete plaques were noted. Table 2 presents the detailed characteristics of the studied arteries and segments.

ESS distribution in the coronary arterial tree

ESS exhibited higher values in the left coronary artery

system than in the right (11.2 Pa vs. 3.7 Pa, $p < 0.001$). The same results occurred when atherosclerotic and non-atherosclerotic segments were studied separately (8.6 Pa vs. 3.4 Pa, $p < 0.05$, and 12.5 Pa vs. 3.8 Pa, $p < 0.001$, respectively). When the left coronary system was separated into the LAD and LCx, the LAD was found to have higher values compared to the LCx and RCA (13.8 Pa vs. 3.5 Pa vs. 3.8 Pa, $p < 0.001$) while there was no significant difference between the LCx and RCA. The same results occurred when atherosclerotic and non-atherosclerotic segments were studied separately (10.1 Pa vs. 4.1 Pa vs. 3.4 Pa, $p < 0.001$, and 15.6 Pa vs. 3.2 Pa vs. 3.8 Pa, $p < 0.001$, respectively).

Table 2. Characteristics of both arteries and segments.

Vessel	n	Arterial length in diastole (mm)	Segments		
			Normal	Diseased	Total
LAD	14 (50%)	63	272 (30%)	149 (16%)	421 (46%)
LCx	5 (18%)	56	94 (10%)	48 (6%)	142 (16%)
RCA	9 (32%)	78	254 (28%)	95 (10%)	349 (38%)
Total	28 (100%)	67	620 (68%)	292 (32%)	912 (100%)

LAD – left anterior descending; LCx – left circumflex; RCA – right coronary artery.

MV distribution in the coronary arterial tree

MV manifested higher values in the left coronary artery system than in the right (0.0027 Pa·s vs. 0.0024 Pa·s, $p < 0.001$). When atherosclerotic and non-atherosclerotic segments were studied separately, the same results occurred in non-atherosclerotic segments (0.0029 Pa·s vs. 0.0024 Pa·s, $p < 0.001$), while in atherosclerotic segments MV was higher in the RCA (0.0025 Pa·s vs. 0.0022 Pa·s, $p < 0.05$). When the left coronary system was divided into the LAD and LCx, LCx was found to have higher values compared to the LAD and RCA (0.0054 Pa·s vs. 0.0017 Pa·s vs. 0.0024 Pa·s, $p < 0.001$). The same results occurred when atherosclerotic and non-atherosclerotic segments were studied separately (0.00343 Pa·s vs. 0.0018 Pa·s vs. 0.0025 Pa·s, $p < 0.001$, and 0.0064 Pa·s vs. 0.0017 Pa·s vs. 0.0024 Pa·s, $p < 0.001$, respectively).

WS distribution in the coronary arterial tree

WS had higher values in the right coronary system artery than in the left (290 mmHg vs. 251 mmHg, $p < 0.001$). When atherosclerotic and non-atherosclerotic segments were studied separately, the same results occurred in non-atherosclerotic segments (320 mmHg vs. 278 mmHg, $p < 0.001$), while in atherosclerotic segments WS was found to be higher in the RCA, but not statistically significantly so (209 mmHg vs. 199 mmHg, $p = 0.115$). When the left coronary system was divided into the LAD and LCx, WS presented higher values in the RCA compared to the LAD and LCx (290 mmHg vs. 256 mmHg vs. 235 mmHg, $p < 0.001$), while there was a trend for a difference between the LAD and LCx ($p = 0.160$). When atherosclerotic and non-atherosclerotic segments were studied separately, the same differences between RCA, LAD and LCx were found in non-atherosclerotic segments (320 mmHg vs. 292 mmHg vs. 237 mmHg, $p < 0.001$). In atherosclerotic segments, WS was higher in the RCA compared to the LAD (209 mmHg vs. 189 mmHg, $p = 0.073$), but the LCx showed higher WS values than the RCA (231 mmHg vs. 209 mmHg, $p < 0.05$).

Curvature distribution in the coronary arterial tree

Curvature demonstrated higher values in the left coronary artery system than in the right (0.128 mm^{-1} vs. 0.123 mm^{-1} , $p < 0.001$). When atherosclerotic and non-atherosclerotic segments were studied separately, the same results occurred in non-atherosclerotic segments (0.120 mm^{-1} vs. 0.118 mm^{-1} , $p < 0.001$),

while in atherosclerotic ones curvature was higher in the left coronary system, but to a non-significant degree (0.145 mm^{-1} vs. 0.136 mm^{-1} , $p = 0.436$). When the left coronary system was divided into the LAD and LCx, curvature presented higher values in the LCx compared to the LAD and RCA (0.145 mm^{-1} vs. 0.123 mm^{-1} vs. 0.123 mm^{-1} , $p < 0.05$), while there was no significant difference between the LAD and RCA ($p = 0.994$). When atherosclerotic and non-atherosclerotic segments were studied separately, the same differences between LCx, LAD and RCA were found in non-atherosclerotic segments (0.143 mm^{-1} vs. 0.112 mm^{-1} vs. 0.119 mm^{-1} , $p < 0.05$). In atherosclerotic segments, curvature was higher in the LCx compared to the LAD and RCA, but only to a non-significant degree (0.149 mm^{-1} vs. 0.143 mm^{-1} vs. 0.136 mm^{-1}).

Torsion distribution in the coronary artery tree

Torsion was found not to differ between any coronary arteries, whether studied overall or in normal and atherosclerotic segments separately. Table 3 summarizes these results.

Discussion

The novelty of this study is the noninvasive assessment of the distribution of ESS, MV, WS, curvature, and torsion within the coronary arterial tree in humans. Hemorrhologic and geometrical factors have been calculated for the left and right coronary arteries *in vivo*, avoiding any distortion by the intravascular ultrasound catheter or complications caused by invasive methods. The study of these parameters in relation to atherosclerosis topography offers a unique opportunity to explain the different incidence of atherosclerosis in various coronary arteries.

It is well established that the atherosclerotic process is associated with low ESS. Low ESS activates

Table 3. Hemorrhologic and geometrical factors in both atherosclerotic and non-atherosclerotic segments.

	ESS (Pa)	MV (Pa·s)	WS (mmHg)	Curvature (mm^{-1})	Torsion (mm^{-1})
LCA	11.2	0.0027	251	0.128	0.0032
LAD	13.8	0.0017	256	0.123	-0.0591
LCx	3.5	0.0054	235	0.145	0.1879
RCA	3.7	0.0024	290	0.123	-0.0150

LCA – left coronary artery system; ESS – endothelial shear stress; MV – molecular viscosity, WS – wall stress. Other abbreviations as in Table 2.

an atherogenic genotypic profile in endothelial cells through special receptors in their membranes, resulting in the promotion of atherosclerosis. Vasoconstrictive substances are overproduced, vasodilatory substances are suppressed, low-density lipoprotein cholesterol permeates to the subendothelial layer at a higher rate, and various proteases and kinases taking part in atherosclerosis are produced.¹²⁻¹³

Epidemiological studies have demonstrated MV to be an independent risk factor for atherosclerosis. The Edinburgh Artery Study has proposed that MV is of the same risk significance as well-known systemic risk factors for cardiovascular disease, such as smoking and hypercholesterolemia. This action is mediated through alterations in blood flow and thrombogenesis.¹⁴⁻¹⁵

There is strong evidence that high WS promotes atherosclerosis. Regions associated with high WS are more susceptible to developing atherosclerosis. Branch origins, which are favorable areas for atherosclerosis development, have higher WS values.¹⁶

Curvature and torsion have recently been studied and are associated with atherosclerosis. High curvature and torsion are considered to boost the atherosclerotic process.¹⁷⁻¹⁸

In our study the LCA was associated with higher values of ESS, lower values of MV, lower values of WS, and smaller curvature than the RCA, while torsion seemed not to differ between them. More specifically, ESS displayed higher values in the LAD compared to the RCA and LCx, while MV showed lower values in the LAD. WS was higher in the RCA compared to the LAD and curvature was greater in the LCx than in the RCA and LAD. These results suggest that atherosclerosis would favor the right rather than the left coronary artery system. However, these results do not conform to the epidemiological data, based on which atherosclerosis is expected to be more frequent in the LAD than in the RCA and LCx. Thus, other factors may affect the different topography of atherosclerosis in the coronary arterial tree, either in isolation or, more likely, in combination with the parameters studied here.

Displacement and axial strain belong among the factors that may affect the difference in topography of atherosclerosis between the LCA and RCA. Displacement is the movement of a material point between two time points. In the case of the coronary arteries, displacement refers to the distance spanned between end-diastole and end-systole. The displacement of the RCA has been found to be twice as great

as that of the LCA, meaning that the velocity of the vessel's motion is respectively higher. This reflects the different location of each vessel on the cardiac surface. This higher displacement of the RCA could affect the topography of atherosclerosis, i.e. it could limit low-density lipoprotein accumulation in the sub-endothelium. Axial strain represents the relative length of a segment and refers to the change in length of an artery during the cardiac cycle: longer in diastole and shorter in systole. A possible difference between the LCA and RCA could affect atherosclerosis and partly explain the different topography.¹⁷⁻¹⁸

The LCA comprises more branches and bifurcations than the RCA. The well-known preference of atherosclerosis for these areas could go some way to explaining the high frequency of atherosclerosis in the LCA. The more branches and bifurcations in an artery, the more likely it is for atherosclerosis to develop. Another potential explanation could be that what matters is the relative change in hemorrheologic and geometric factors, and not the absolute values. For example, a higher ESS in a region in the LAD could be atheroprotective compared to an adjacent region with low ESS, although it might be lower than the ESS in the RCA. It is possible that pulsatile flow, observed mainly in the LCA, induces low and oscillatory ESS to a greater extent than in the RCA, resulting in the onset of atherosclerosis.¹⁹

Study limitations

The study calculations were performed for 2-mm long segments, and thus did not investigate more subtle variations of the study parameters along the coronary arteries. The study population was limited, which affects the generalizability of our results; however, this study may serve as a proof-of-concept and a demonstration of methodological feasibility for subsequent large-scale, multiple-time-point analyses. The cross-sectional nature of our study does not permit the demonstration of causal relationships between the associated variables.

Conclusions

This study assessed noninvasively the possible differences in flow dynamics and geometry between the left and right coronary arterial system in humans *in vivo*, attempting to explain in a pathophysiological way the more frequent appearance of atherosclerosis in the LAD. The study revealed significant differences in

ESS, MV, WS, and curvature, but not in a way that could explain the heterogeneous distribution pattern of atherosclerosis. Other parameters, either alone or in combination with those evaluated here, may be implicated in the differences in atherosclerosis topography manifested clinically.

Acknowledgements

Special thanks to Prof. J. Soulis and to Y. Chatzizisis for their consultative role.

References

1. Giannoglou GD, Antoniadis AP, Chatzizisis YS, Louridas GE. Difference in the topography of atherosclerosis in the left versus right coronary artery in patients referred for coronary angiography. *BMC Cardiovasc Disord.* 2010; 10: 26.
2. Tuzcu EM, Kapadia SR, Tutar E, et al. High prevalence of coronary atherosclerosis in asymptomatic teenagers and young adults: evidence from intravascular ultrasound. *Circulation.* 2001; 103: 2705-2710.
3. Montenegro MR, Eggen DA. Topography of atherosclerosis in the coronary arteries. *Lab Invest.* 1968; 18: 586-593.
4. Asakura T, Karino T. Flow patterns and spatial distribution of atherosclerotic lesions in human coronary arteries. *Circ Res.* 1990; 66: 1045-1066.
5. Malek AM, Alper SL, Izumo S. Hemodynamic shear stress and its role in atherosclerosis. *JAMA.* 1999; 282: 2035-2042.
6. Schroeder S, Kopp AF, Baumbach A, et al. Noninvasive detection and evaluation of atherosclerotic coronary plaques with multislice computed tomography. *J Am Coll Cardiol.* 2001; 37: 1430-1435.
7. Katranas SA, Kelekis AL, Antoniadis AP, et al. Non-invasive assessment of endothelial shear stress and coronary stiffness using multislice computed tomography. *Int J Cardiol.* 2011; 152: 281-284.
8. Coskun AU, Yeghiazarians Y, Kinlay S, et al. Reproducibility of coronary lumen, plaque, and vessel wall reconstruction and of endothelial shear stress measurements in vivo in humans. *Catheter Cardiovasc Interv.* 2003; 60: 67-78.
9. Perktold K, Nerem RM, Peter RO. A numerical calculation of flow in a curved tube model of the left main coronary artery. *J Biomech.* 1991; 24: 175-189.
10. Matsuo S, Tsuruta M, Hayano M, et al. Phasic coronary artery flow velocity determined by Doppler flowmeter catheter in aortic stenosis and aortic regurgitation. *Am J Cardiol.* 1988; 62: 917-922.
11. Soulis JV, Giannoglou GD, Chatzizisis YS, Seralidou KV, Parcharidis GE, Louridas GE. Non-Newtonian models for molecular viscosity and wall shear stress in a 3D reconstructed human left coronary artery. *Med Eng Phys.* 2008; 30: 9-19.
12. Reneman RS, Arts T, Hoeks AP. Wall shear stress--an important determinant of endothelial cell function and structure--in the arterial system in vivo. Discrepancies with theory. *J Vasc Res.* 2006; 43: 251-269.
13. Chatzizisis YS, Coskun AU, Jonas M, Edelman ER, Stone PH, Feldman CL. Risk stratification of individual coronary lesions using local endothelial shear stress: a new paradigm for managing coronary artery disease. *Curr Opin Cardiol.* 2007; 22: 552-564.
14. Lowe GD, Lee AJ, Rumley A, Price JF, Fowkes FG. Blood viscosity and risk of cardiovascular events: the Edinburgh Artery Study. *Br J Haematol.* 1997; 96: 168-173.
15. Kwaan HC. Role of plasma proteins in whole blood viscosity: a brief clinical review. *Clin Hemorheol Microcirc.* 2010; 44: 167-176.
16. Thubrikar MJ, Robicsek F. Pressure-induced arterial wall stress and atherosclerosis. *Ann Thorac Surg.* 1995; 59: 1594-1603.
17. Ding Z, Friedman MH. Dynamics of human coronary arterial motion and its potential role in coronary atherogenesis. *J Biomech Eng.* 2000; 122: 488-492.
18. Zhu H, Friedman MH. Relationship between the dynamic geometry and wall thickness of a human coronary artery. *Arterioscler Thromb Vasc Biol.* 2003; 23: 2260-2265.
19. Chatzizisis YS, Giannoglou GD, Parcharidis GE, Louridas GE. Is left coronary system more susceptible to atherosclerosis than right? A pathophysiological insight. *Int J Cardiol.* 2007; 116: 7-13.